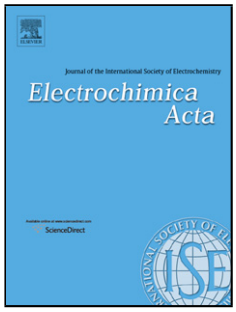

Title: Platinum Nanoparticles Encapsulated in Carbon Microspheres: Toward Electro-Catalyzing Glucose with High Activity and Stability

Author: Xiangheng Niu Hongli Zhao Minbo Lan Liang Zhou

PII: S0013-4686(14)02201-4
DOI: http://dx.doi.org/doi:10.1016/j.electacta.2014.11.024
Reference: EA 23696

To appear in: *Electrochimica Acta*

Received date: 10-10-2014
Revised date: 4-11-2014
Accepted date: 5-11-2014

Please cite this article as: Xiangheng Niu, Hongli Zhao, Minbo Lan, Liang Zhou, Platinum Nanoparticles Encapsulated in Carbon Microspheres: Toward Electro-Catalyzing Glucose with High Activity and Stability, Electrochimica Acta http://dx.doi.org/10.1016/j.electacta.2014.11.024

Platinum Nanoparticles Encapsulated in Carbon Microspheres: Toward Electro-Catalyzing Glucose with High Activity and Stability

Xiangheng Niu,[a] Hongli Zhao,[a] Minbo Lan,[a, b, *] Liang Zhou[c]

[a] Shanghai Key Laboratory of Functional Materials Chemistry, East China University of Science and Technology, Shanghai 200237, PR China

[b] State Key Laboratory of Bioreactor Engineering, East China University of Science and Technology, Shanghai 200237, PR China

[c] Australian Institute of Bioengineering and Nanotechnology, University of Queensland, Brisbane QLD4072, Australia

* Corresponding author. E-mail: minbolan@ecust.edu.cn

Highlights

- Synthesis of Pt NPs dispersedly encapsulated in carbon microspheres;
- Reduced glutathione (R-GSH) as the capping agent and reductant simultaneously;
- Showing high electrocatalytic activity for glucose oxidation in neutral media;
- Possessing attractive stability of performance due to the

carbon-encapsulated structure.

Abstract

Electro-oxidizing glucose effectively is well known as the critical point in developing analytical sensors and carbohydrate-based fuel cells. Here we prepared a new electrode material, platinum nanoparticles encapsulated in carbon microspheres (Pt/GSH), to promote the glucose electrocatalytic oxidation reaction in neutral media. The Pt/GSH composite was synthesized by using a simple hydrothermal method, with reduced glutathione (R-GSH) as the capping agent and reductant simultaneously, followed by a calcination process. It was found that the obtained Pt particles with a mean size of 26.8 nm were well dispersed in the interconnected carbon microspheres, providing a stable and efficient catalytic platform for glucose electro-oxidation. As a result, the synthesized catalyst exhibited higher activity for electro-catalyzing glucose compared to commercial Pt black and Pt/C catalysts, with a mass activity of 15.4 μA μg^{-1}_{Pt}, approximately 13 times of Pt black and 2.1 times of Pt/C. Besides, due to the decreased dissolution and agglomeration of Pt NPs in the carbon-encapsulated structure, the Pt/GSH catalyst kept quite stable activity upon reuse even in the presence of chloride ions.

Keywords: Pt NPs encapsulated in carbon microspheres; Electrocatalysis; Glucose oxidation; High mass activity; Stability

1. Introduction

Electro-catalyzing the glucose oxidation reaction turns to be a research focus in the academic field due to its wide promising applications in heterogeneous catalysis [1-3], biofuel cells [4,5] and analytical sensors [6-8]. In the past few years, several materials including noble metals (Pt, Pd, Au, et al.) [6,9-11], non-precious metals (Ni, Cu, et al.) [12-14], and non-metallic electrodes [15,16] have been explored to promote this sluggish kinetics-controlled reaction. Among these materials, Pt is generally believed to be the most effective and stable catalyst candidate [17-19]. However, the following two critical issues seriously hinder the industrial use of Pt-based catalysts on a large scale: first, the glucose oxidation reaction occurred on conventional Pt electrodes can not produce sufficient faradic current responses for various utilizations; second, the catalytic activity of Pt materials is easily poisoned by species such as chloride ions. Therefore, there is still a huge demand for developing new catalysts with favorable activity and stability for the glucose electro-oxidation reaction.

Here we report the synthesis of a new high-efficiency catalyst, Pt nanoparticles dispersedly encapsulated in carbon microspheres (denoted as Pt/GSH), to facilitate the electrocatalytic oxidation of glucose in neutral media. In this synthesis, reduced glutathione (R-GSH) was employed as the reducing agent as well as capping agent for the first time.

The resulting Pt particles with a mean size of 26.8 nm were well dispersed in the interconnected carbon spheres, providing a stable and efficient catalytic platform for glucose electro-oxidation. As a result, the prepared catalyst exhibited much higher activity and preferable stability for electro-catalyzing glucose in the presence of chloride ions compared to commercial Pt black and Pt/C catalysts.

2. Experimental

2.1. Chemicals

K_2PtCl_4 and D-glucose were purchased from Shanghai Aladdin Reagent Co. R-GSH was provided by Sigma-Aldrich. H_2SO_4, KH_2PO_4, K_2HPO_4, and KCl were received from Sinopharm Chemical Reagent Co., Ltd. Glucose stock solutions were allowed to mutarotate overnight before use. Ultrapure water (18.2 MΩ•cm, Laboratory Water Purification Systems) was utilized in all experiments. All other chemicals used were at least of analytical grade.

2.2. Synthesis of the Pt/GSH catalyst

In a typical synthesis, firstly, 0.154 g R-GSH (25 mM) was fully dissolved with 18 mL ultrapure water; then 2 mL of 50 mM K_2PtCl_4 stock solution was added into the R-GSH solution quickly under stirred conditions (the concentration of K_2PtCl_4 was determined to be 5 mM); after mixing within 5 min, the mixture was transferred into a stainless solvothermal reactor with PTFE inner for reaction for 12 h under 180 ^oC;

after reaction, the Pt/GSH product was collected by centrifugation and water-washing alternately; afterwards, the obtained composite was calculated at 400 ^{o}C under a N_2 atmosphere for 4 h; finally, the prepared catalyst was used for characterization and electrochemical tests.

2.3. Characterization

The TEM images were captured on a JSM-1400 transmission electron microscope (JEOL, Japan) with an accelerating voltage of 100 kV; The EDS and elemental mapping patterns were obtained using a XM-2 energy disperse spectrometer (EDAX, USA) equipped to a JSM-2100 TEM (JEOL, Japan). The XRD measurement was performed on a D/MAX2550 diffractometer (Rigaku International Co., Japan) using Cu Kα radiation (λ = 0.15408 nm) at a scan rate of 0.2^{o} per minute. The XPS measurement was carried out on an ESCALAB 250Xi X-ray photoelectron spectrometer (Thermo Fisher, USA). The N_2 adsorption-desorption test was implemented on an automatic ASAP2020 analyzer (Micromeritics Instrument Co., USA). The ICP-OES method performed on an IRIS-1000 inductively coupled plasma optical emission spectroscope (Thermo Elemental, USA) was used to determine the precise mass of Pt encapsulated in carbon microspheres.

2.4. Electrochemical measurements

All electrochemical experiments were carried out on a CHI440A electrochemical workstation (CH Instruments Inc., USA) equipped with a

conventional three-electrode configuration consisting of a catalyst-modified screen-printed carbon working electrode (SPCE) [20], a Pt wire counter electrode and a 3 M KCl saturated Ag/AgCl reference electrode. Unless otherwise states, all potentials reported were referred to the saturated Ag/AgCl electrode at room temperature. All cyclic voltammetric and chronoamperometric measurements in the present study were performed in stationary electrolyte solutions.

3. Results and discussion

3.1. Synthesis and characterization of the Pt/GSH catalyst

(Please inset Figure 1 here)

The proposed Pt/GSH was fabricated using a facile method combining rough hydrothermal synthesis with subsequent calcination. Figure 1 illustrates the fabrication procedure of Pt/GSH. First, the $PtCl_4^{2-}$ precursor and R-GSH are adequately mixed and transferred for hydrothermal reaction. During the hydrothermal treatment, the R-GSH acts as the reductant, reducing Pt^{II} to Pt particles under high temperatures, and the R-GSH itself is oxidized to glutathione (O-GSH). As far as we know, this is the first example of utilizing GSH to reduce noble metal precursors to synthesize nanomaterials. Meanwhile, the R-GSH also acts as a capping agent to inhibit Pt crystal overgrowth and aggregation [21-23]. By self-assembling into biomolecule micelles, the Pt nanoparticles can be encapsulated within them. Transmission electron microscopy (TEM)

images, as shown in Figure 2A, demonstrate that spherical composites with an average diameter of 1.35 μm are obtained. These colloids show some aggregation by connecting each other because of the electrostatic interaction [21]. What needs to be noted is that Pt particles cannot be well recognized from the TEM image, because the microspheres are too thick for stimulated electron transmission. While the energy dispersive spectroscopy (EDS) and elemental mapping patterns (Figure 2B-F) confirm the presence of Pt highly dispersed in these colloidal microspheres. In addition, the characteristic signal of S derived from GSH is also observed. The obtained composites are then calcined under an inert atmosphere. The high-temperature carbonization process has little effects on the morphology of these spheres and the dispersity of Pt, as demonstrated by Figure 2G and Figure 2H-L, but shrinks the microsphere size to 950 nm.

(Please inset Figure 2 here)

Figure 3A depicts the X-ray diffraction (XRD) pattern of the resulting Pt/GSH catalyst. It provides three remarkable diffraction peaks located at 2θ values of 39.80°, 46.28°, and 67.54°, which are well assigned to the (111), (200), and (220) planes of the face-centered cubic Pt crystal structure (JCPDS card 65-2868), respectively. According to the values of the full-width at half-maximum (FWHM) of the (111) and (200) diffraction peaks, the mean crystallite size of Pt particles is calculated to

be 26.8 nm by Scherrer equation ($D = 0.89\lambda/\beta\cos\theta$, where D is the particle size, λ is the radiation wavelength, β is the FWHM, and θ is the Bragg diffraction angle) [24,25]. X-ray photoelectron spectroscopy (XPS) shown in Figure 3B further confirms that the surface of Pt nanoparticles is composed of metallic Pt. The characteristic peaks centered at 71.4 and 74.7 eV are attributed to $Pt4f_{7/2}$ and $Pt4f_{5/2}$, respectively, agreeing with those published elsewhere [26]. The content of Pt evaluated by inductively coupled plasma optical emission spectroscopy (ICP-OES) is found to be 13.9 wt% in the synthesized Pt/GSH catalyst. Furthermore, the N_2 adsorption-desorption isotherms (Figure 3C) reveal that the Pt nanoparticle-encapsulated carbon microspheres present a porous structure, which is caused by dehydrogenation and deoxygenation from the polymeric frameworks during the high-temperature pyrolysis [27]. The Brunauer-Emmett-Teller (BET) surface area is determined to be 46.5 $m^2 g^{-1}$. This porous architecture is thought to be much beneficial for the reactant to diffuse to active sites and for the product to escape away from the electrode surface timely [28,29].

(Please inset Figure 3 here)

3.2. Electrocatalysis of glucose at Pt/GSH

(Please inset Figure 4 here)

In this study, the catalytic properties of the prepared Pt/GSH towards glucose electro-oxidation in neutral solutions were systematically

evaluated. For comparison, two commercial catalysts, Pt black (Sigma-Aldrich, 10 nm particles) and Pt/C (Johnson Matthey, 20 wt% Pt particles with a size of ＜3.5 nm on Vulcan XC-72 carbon support), were also checked under identical conditions. Figure 4 represents the stable cyclic voltammograms (CVs) of the three catalysts in 0.5 M deoxygenized H_2SO_4. It is found that all catalysts provide a notable cathodic peak at around +0.5 V vs. Ag/AgCl, attributing to the reduction response of Pt oxide. As expected, in the potential region of -0.2～+0.1 V, two pairs of reversible peaks with a little overlap are noticed, corresponding to the hydrogen adsorption/desorption processes on the Pt-modified electrode surface. The electrochemically active surface area (ECSA), which is calculated by collecting the hydrogen adsorption/desorption charge after double-layer correction [30], is found to be 64.6 $m^2 g^{-1}$ for Pt/GSH, slightly larger than that of Pt/C (56.4 $m^2 g^{-1}$), and 6.7 times of the Pt black catalyst. As for the Pt/GSH catalyst with larger particle size compared to Pt/C, the excellent dispersibility of Pt NPs may play a non-ignorable role in providing the comparable ECSA. This large ECSA of Pt/GSH is supposed to provide abundant active sites for the electro-oxidation reaction of glucose.

(Please inset Figure 5 here)

Figure 5A displays CVs of the proposed Pt/GSH catalyst in phosphate buffer solution (PBS, pH 7.4) containing 0.15 M chloride ions. Similar to

Pt black and Pt/C (Figure S1 and S2 in Supporting Information) the Pt/GSH modified electrode exhibits current responses of glucose oxidation in three distinctive potential regions. The blank GSH without Pt loading provides the same CVs for the absence and presence of glucose (data not shown), demonstrating that the electrocatalytic ability for glucose oxidation originates from noble metal Pt. In the hydrogen region the chemisorption and dehydrogenation of glucose generate a peak at $<$ -0.3 V, and the chemisorbed species after the removal of the first hydrogen atom are further electro-oxided in the double-layer scope, providing a peak centered at -0.15 V; the response starting at approximately +0.4 V derives from the oxidation of glucose by PtO in the oxygen region [31]. Based on the current response at -0.15 V, the determined sensitivity of Pt/GSH is up to 0.74 μA $mM^{-1}_{glucose}$ μg^{-1}_{Pt}, much higher than that of Pt black (0.04 μA $mM^{-1}_{glucose}$ μg^{-1}_{Pt}) and Pt/C (0.35 μA $mM^{-1}_{glucose}$ μg^{-1}_{Pt}). The chronoamperometric technique was used to assess the activity of the fabricated Pt/GSH catalyst. As depicted in Figure 5B, it is found that the Pt/GSH possesses better catalytic ability for the glucose electro-oxidation reaction compared to Pt black and Pt/C, with a mass activity of 15.4 μA μg^{-1}_{Pt}, approximately 13 times of Pt black (1.2 μA μg^{-1}_{Pt}) and 2.1 times of Pt/C (7.5 μA μg^{-1}_{Pt}). This improved catalytic activity of Pt/GSH may result from the beneficial large ECSA and the porous microsphere structure, which allows species to transfer on the

electrode interface freely.

Apart from the catalytic activity, the ability of remaining active for Pt-based catalysts is also of great importance. In the present work, we recorded the changes of the activity of Pt/GSH, Pt black, and Pt/C catalysts over the times of reuse in solutions with the presence of 0.15 M chlorides ions, as shown in Figure 6. Obviously, the Pt/GSH exhibits better stability of activity in comparison with the Pt black and Pt/C catalysts. After 100 cycles, the proposed Pt/GSH still retains fairly high activity, with only a 3.4% loss of catalytic activity. While the commercial Pt black and Pt/C catalysts lose their activities to 83.4% and 85.8%, respectively. The better active stability of Pt/GSH is mainly attributed to the following reasons: compared to the small size of Pt particles in Pt black (～10 nm) and Pt/C (less than 3.5 nm), the larger size of Pt nanoparticles in Pt/GSH (a mean size of 26.8 nm estimated by the Scherrer equation) endows lower interfacial free energy [32], thus slowing down the poisonous species Cl^- to block the electroactive surface [33,34]; more importantly, these porous sulfur-doped carbon microspheres can act as cages and well encapsulate the Pt nanoparticles in them, significantly reducing the electrochemical dissolution and agglomeration of Pt NPs [35,36].

(Please inset Figure 6 here)

4. Conclusions

In conclusion, we have demonstrated a simple yet efficient approach to prepare Pt nanoparticles dispersedly encapsulated in carbon microspheres, involving the reduction synthesis and encapsulation of Pt particles using R-GSH as both the reductant and the capping agent, and the subsequent carbonization process in an inert atmosphere. The resulting Pt/GSH presents favorable activity for electro-catalyzing glucose in neutral media, 13 and 2.1 times mass activity of commercial Pt black and Pt/C catalysts, respectively. Besides, the Pt/GSH catalyst keeps quite stable activity upon reuse even in the presence of chloride ions. Due to its facile and reproducible synthesis and favorable catalytic properties, the proposed material would find wider applications in the catalysis of hydrogen oxidation, oxygen reduction, and other reactions. Also, this study enriches the resource of optional reducing-capping agents in controllable synthesis of nanocrystals.

Acknowledgments

This work was financially supported by the NSFC (21305044), the Science and Technology Commission of Shanghai Municipality (13510710900), and the Fundamental Research Funds for the Central Universities (222201314026).

References

[1] B. Seo, S. Choi, J. Kim, Simple electrochemical deposition of Au nanoplates from Au(I) cyanide complexes and their electrocatalytic

activities, ACS Applied Materials & Interfaces 3 (2011) 441.

[2] X.H. Niu, M.B. Lan, H.L. Zhao, C. Chen, Well-dispersed Pt cubes on porous Cu foam: high-performance catalysts for the electrochemical oxidation of glucose in neutral media, Chemistry–A European Journal 19 (2013) 9534.

[3] J.W. Zhao, X.G. Kong, W.Y. Shi, M.F. Shao, J.B. Han, M. Wei, D.G. Evans, X. Duan, Self-assembly of layered double hydroxide nanosheets/Au nanoparticles ultrathin films for enzyme-free electrocatalysis of glucose, Journal of Materials Chemistry 21 (2011) 13926.

[4] K. Elouarzaki, A.L. Goff, M. Holzinger, J. Thery, S. Cosnier, Electrocatalytic oxidation of glucose by rhodium porphyrin-functionalized MWCNT electrodes: application to a fully molecular catalyst-based glucose/O_2 fuel cell, Journal of the American Chemistry Society 134 (2012) 14078.

[5] A. Kloke, C. Köhler, R. Zengerle, S. Kerzenmacher, Porous platinum electrodes fabricated by cyclic electrodeposition of PtCu alloy: application to implantable glucose fuel cells, The Journal of Physical Chemistry C 116 (2012) 19689.

[6] L. Meng, J. Jin, G.X. Yang, T.H. Lu, H. Zhang, C.X. Cai, Nonenzymatic electrochemical detection of glucose based on

palladium–single-walled carbon nanotube hybrid nanostructures, Analytical Chemistry 81 (2009) 7271.

[7] Y. Yamauchi, A. Tonegawa, M. Komatsu, H.J. Wang, L. Wang, Y. Nemoto, N. Suzuki, K. Kuroda, Electrochemical synthesis of mesoporous Pt-Au binary alloys with tunable compositions for enhancement of electrochemical performance, Journal of the American Chemistry Society 134 (2012) 5100.

[8] C.L. Li, H.J. Wang, Y. Yamauchi, Electrochemical deposition of mesoporous Pt-Au alloy films in aqueous surfactant solutions: towards a highly sensitive amperometric glucose sensor, Chemistry–A European Journal 19 (2013) 2242.

[9] J.H. Yuan, K. Wang, X.H. Xia, Highly ordered platinum-nanotubule arrays for amperometric glucose sensing, Advanced Functional Materials 15 (2005) 803.

[10] H. Zhang, J.J. Xu, H.Y. Chen, Shape-controlled gold nanoarchitectures: synthesis, superhydrophobicity, and electrocatalytic properties, The Journal of Physical Chemistry C 112 (2008) 13886.

[11] H.Y. Bai, M. Han, Y.Z. Du, J.C. Bao, Z.H. Dai, Facile synthesis of porous tubular palladium nanostructures and their application in a nonenzymatic glucose sensor, Chemical Communications 46 (2010) 1739.

[12] Z.J. Luo, S. Yin, J. Wang, H.M. Li, L.G. Wang, H. Xu, J.X. Xia,

Synthesis of one-dimensional β-$Ni(OH)_2$ nanostructure and their application as nonenzymatic glucose sensors, Materials Chemistry and Physics 132 (2012) 387.

[13] H. Pang, Q.Y. Lu, J.J. Wang, Y.C. Li, F. Gao, Glucose-assisted synthesis of copper micropuzzles and their application as nonenzymatic glucose sensors, Chemical Communications 46 (2010) 2010.

[14] X.J. Zhang, G.F. Wang, A.X. Gu, Y. Wei, B. Fang, CuS nanotubes for ultrasensitive nonenzymatic glucose sensors, Chemical Communications (2008) 5945.

[15] D.B. Luo, L.Z. Wu, J.F. Zhi, Fabrication of boron-doped diamond nanorod forest electrodes and their application in nonenzymatic amperometric glucose biosensing, ACS Nano 3 (2009) 2121.

[16] Q. Wang, P. Subramanian, M. Li, W.S. Yeap, K. Haenen, Y. Coffinier, R. Boukherroub, S. Szunerits, Non-enzymatic glucose sensing on long and short diamond nanowire electrodes, Electrochemistry Communications 34 (2013) 286.

[17] L. Wang, Y. Yamauchi, Controlled aqueous solution synthesis of platinum-palladium alloy nanodendrites with various compositions using amphiphilic triblock copolymers, Chemistry-An Asian Journal 5 (2010) 2493.

[18] H.J. Wang, L. Wang, T. Sato, Y. Sakamoto, S. Tominaka, K. Miyasaka, N. Miyamoto, Y. Nemoto, O. Terasaki, Y. Yamauchi, Synthesis of mesoporous Pt films with tunable pore sizes from aqueous surfactant solutions, Chemistry of Materials 24 (2012) 1591.

[19] C.L. Li, T. Sato, Y. Yamauchi, Electrochemical synthesis of one-dimensional mesoporous Pt nanorods using the assembly of surfactant micelles in confined space, Angewandte Chemie International Edition 52 (2013) 8050.

[20] X.H. Niu, C. Chen, H.L. Zhao, J. Tang, Y.X. Li, M.B. Lan, Porous screen-printed carbon electrode, Electrochemistry Communications 22 (2012) 170.

[21] Z.Q. Niu, Y.D. Li, Removal and utilization of capping agents in nanocatalysis, Chemistry of Materials 26 (2014) 72.

[22] N. Sakai, T. Tatsuma, One-step synthesis of glutathione-protected metal (Au, Ag, Cu, Pd, and Pt) cluster powders, Journal of Materials Chemistry A 1 (2013) 5915.

[23] S.E. Eklund, D.E. Cliffel, Synthesis and catalytic properties of soluble platinum nanoparticles protected by a thiol monolayer, Langmuir 20 (2004) 6012.

[24] Y. Zhao, F. Li, R. Zhang, D.G. Evans, X. Duan, Preparation of layered double-hydroxide nanomaterials with a uniform crystallite size

using a new method involving separate nucleation and aging steps, Chemistry of Materials 14 (2002) 4286.

[25] H. Borchert, E.V. Shevchenko, A. Robert, I. Mekis, A. Kornowski, G. Grübel, H. Weller, Determination of nanocrystal sizes: a comparison of TEM, SAXS, and XRD studies of highly monodisperse $CoPt_3$ particles, Langmuir 21 (2005) 1931.

[26] S.H. Sun, D.Q. Yang, D. Villers, G.X. Zhang, E. Sacher, J.P. Dodelet, Template- and surfactant-free room temperature synthesis of self-sssembled 3D Pt nanoflowers from single-crystal nanowires, Advanced Materials 20 (2008) 571.

[27] S.S. Feng, W. Li, Q. Shi, Y.H. Li, J.C. Chen, Y. Ling, A.M. Asiri, D.Y. Zhao, Synthesis of nitrogen-doped hollow carbon nanospheres for CO_2 capture, Chemical Communications 50 (2014) 329.

[28] H.C. Shin, J. Dong, M.L. Liu, Nanoporous structures prepared by an electrochemical deposition process, Advanced Materials 15 (2003) 1610.

[29] H.C. Shin, M.L. Liu, Three-dimensional porous copper-tin alloy electrodes for rechargeable lithium batteries, Advanced Functional Materials 15 (2005) 582.

[30] B. Lim, M.J. Jiang, P.H.C. Camargo, E.C. Cho, J. Tao, X.M. Lu, Y.M. Zhu, Y.N. Xia, Pd-Pt bimetallic nanodendrites with high activity for oxygen reduction, Science 324 (2009) 1302.

[31] K.E. Toghill, R.G. Compton, Electrochemical non-enzymatic glucose sensors: a perspective and an evaluation, International Journal of Electrochemical Sciences 5 (2010) 1246.

[32] C. Wang, H. Daimon, T. Onodera, T. Koda, S.H. Sun, A general approach to the size- and shape-controlled synthesis of platinum nanoparticles and their catalytic reduction of oxygen, Angewandte Chemie International Edition 47 (2008) 3588.

[33] J.P. Wang, D.F. Thomas, A.C. Chen, Nonenzymatic electrochemical glucose sensor based on nanoporous PtPb networks, Analytical Chemistry 80 (2008) 997-1004.

[34] N. Job, M. Chatenet, S. Berthon-Fabry, S. Hermans, F. Maillard, Efficient Pt/carbon electrocatalysts for proton exchange membrane fuel cells: avoid chloride-based Pt salts!, Journal of Power Sources 240 (2013) 294-305.

[35] Q. Zhang, I. Lee, J.B. Joo, F. Zaera, Y.D. Yin, Core-shell nanostructured catalysts, Accounts of Chemical Research 46 (2013) 1816.

[36] A.K. Schuppert, A. Savan, A. Ludwig, K.J.J. Mayrhofer, Potential-resolved dissolution of Pt-Cu: a thin-film material library study, Electrochimica Acta 144 (2014) 332.

Figure captions

Figure 1. Schematic illustration of the formation process of Pt/GSH.

Figure 2. TEM images (A and G), EDS patterns (B and H), and elemental mapping images (C-F and I-L) of the Pt/GSH before (A-F) and after (G-L) calcination.

Figure 3. (A) XRD pattern of the Pt/GSH catalyst, (B) High-resolution XPS pattern for the Pt4f region of the synthesized Pt/GSH, and (C) N_2 adsorption-desorption isotherms of the synthesized Pt/GSH.

Figure 4. Stable CVs of commercial Pt black, Pt/C, and the synthesized Pt/GSH in 0.5 M H_2SO_4 solution recorded at a scan rate of 20 mV s^{-1}.

Figure 5. (A) CVs of the Pt/GSH catalyst in 0.1 M PBS (pH 7.4) + 0.15 M KCl solution with the absence and presence of 5 mM glucose. Scan rate: 50 mV s^{-1}; (B) I-t curves of the three catalysts in 0.1 M PBS (pH 7.4) containing 0.15 M KCl and 10 mM glucose after background subtraction. Applied potential: -0.15 V vs. Ag/AgCl.

Figure 6. Changes of the catalytic activity of the three catalysts over the times of their recycling use.

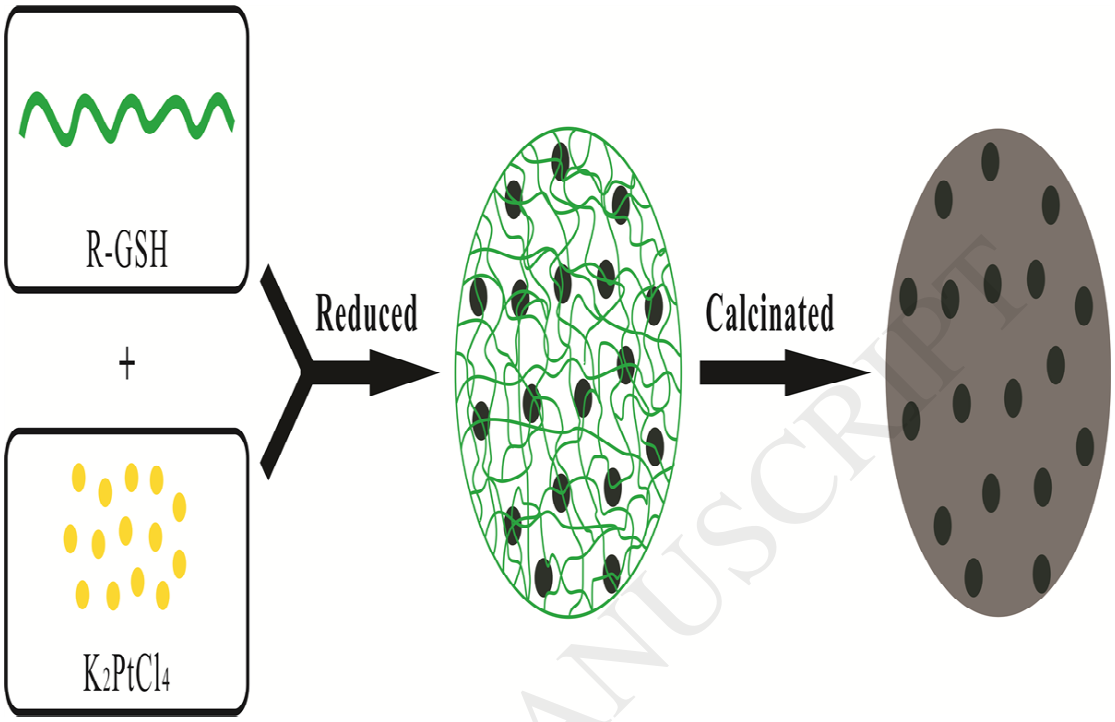

Figure 1 .

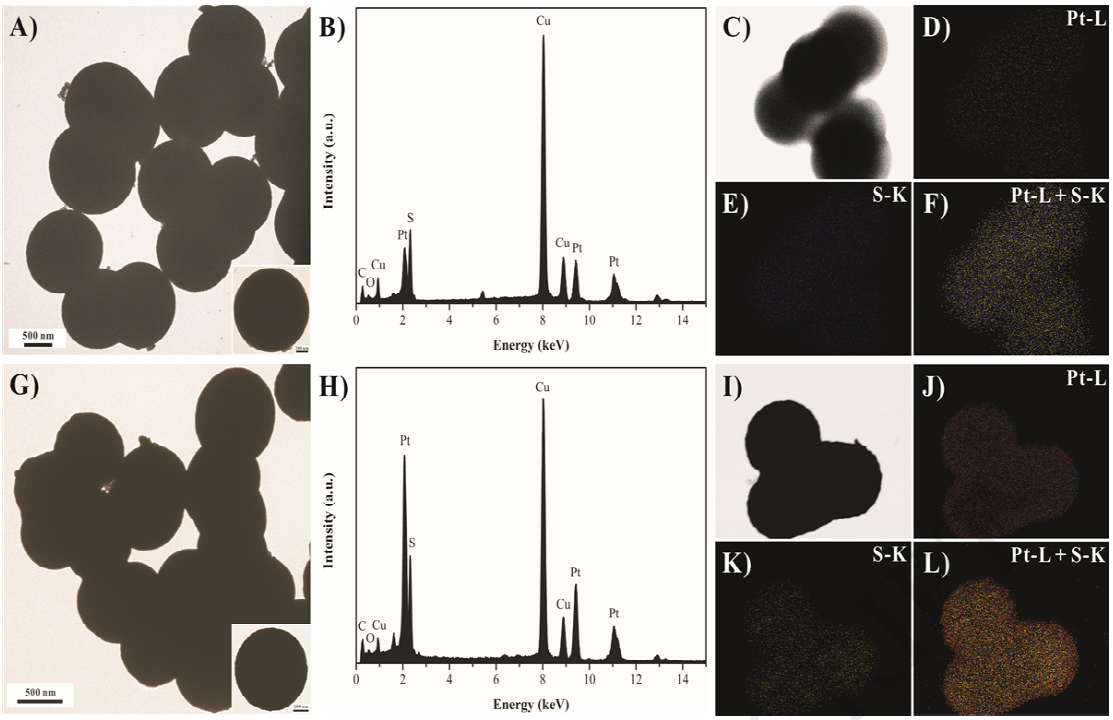

Figure 2 .

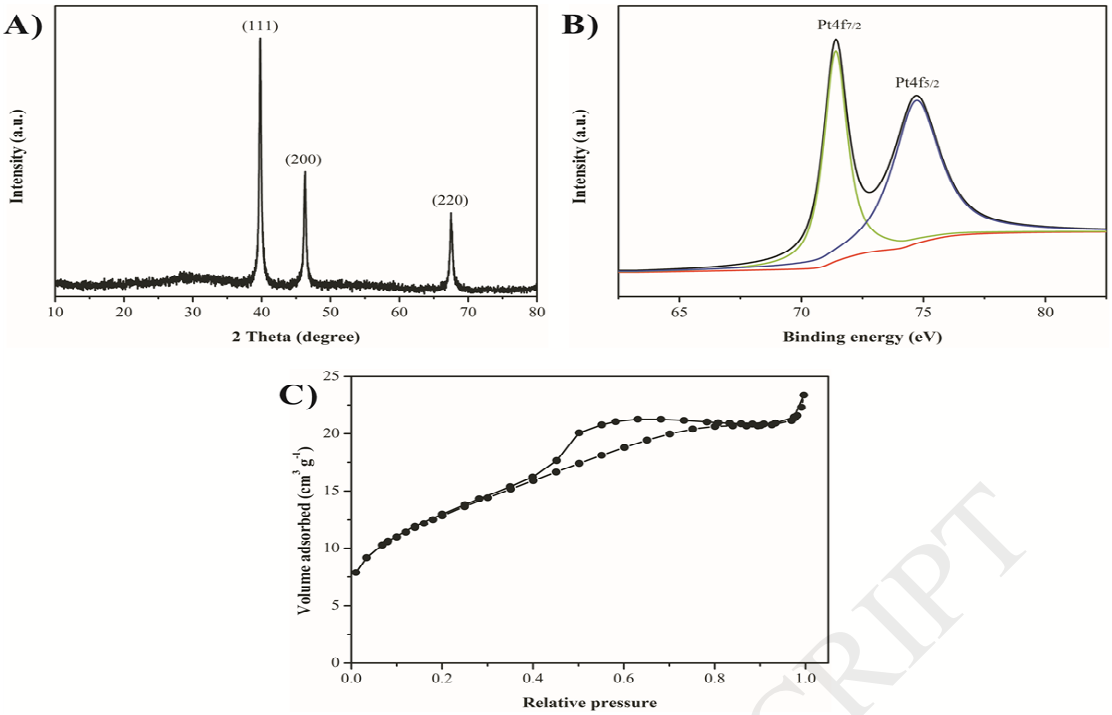

Figure 3 .

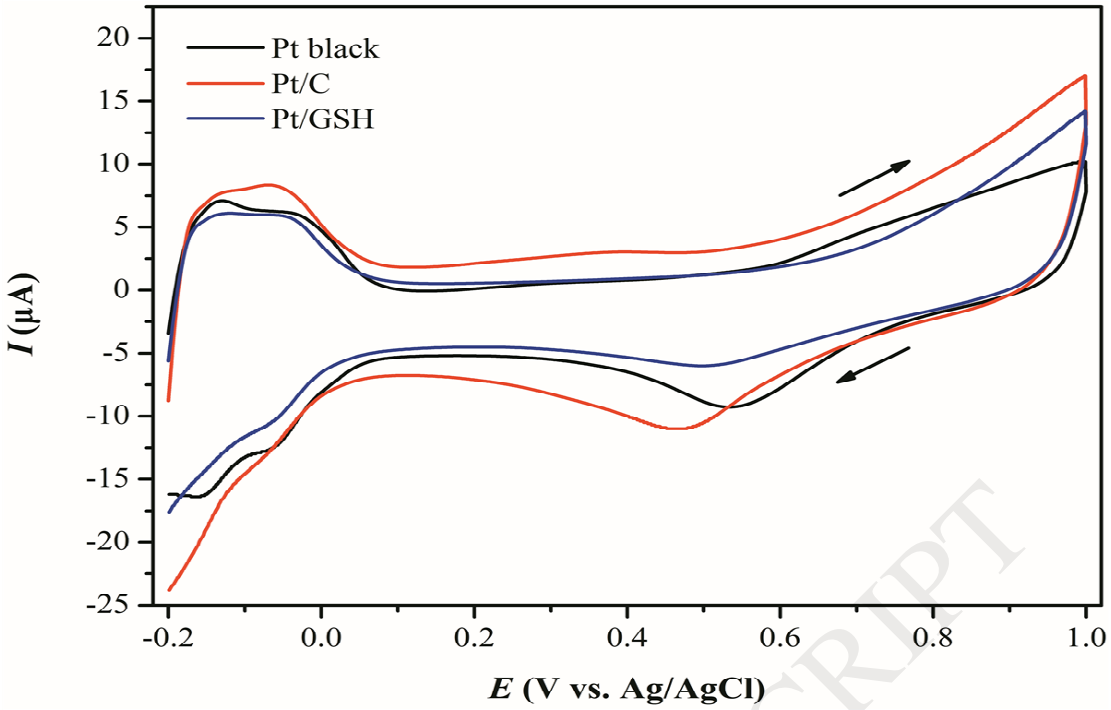

Figure 4 .

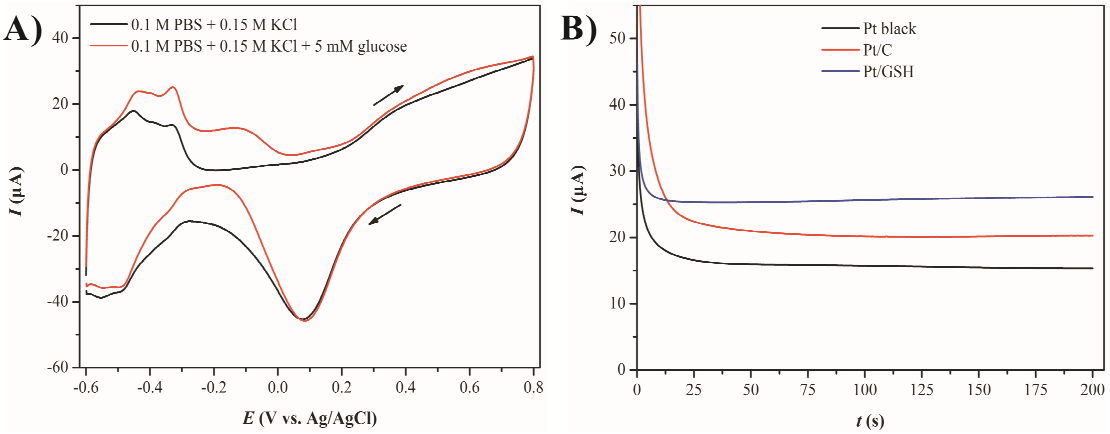

Figure 5 .

Figure 6 .

Graphical abstract .